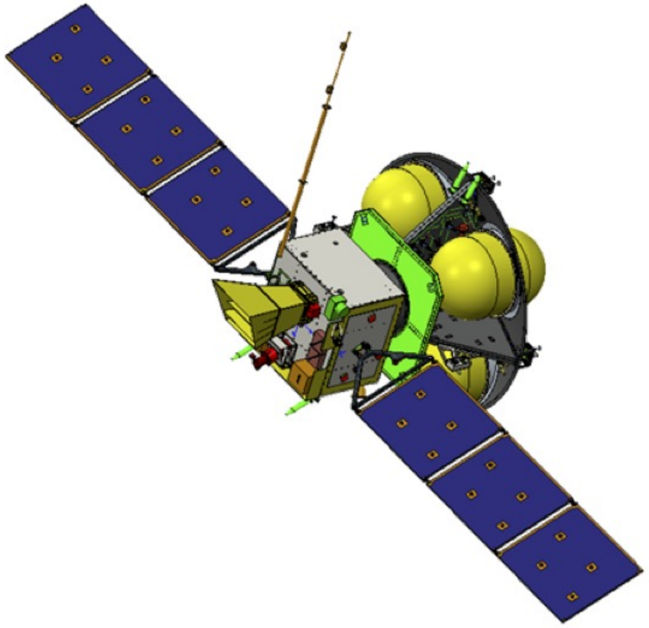

The Soft X-ray Imager (SXI) on the SMILE Mission: Description and Ground Calibration (to date)

Dr. Steven Sembay
SXI PI
University of Leicester

Thanks to the SMILE and SXI consortium for material provided

The Soft X-ray Imager (SXI) on the SMILE Mission

S. Sembay[1], A. L. Alme[5], T. Arnold[4], A. Beardmore[1], A. Belén Balado Margeli[8], C. Bicknell[1,2], C. Bouldin[2], G. Branduardi-Raymont[3], J. P. Breuer[20], T. Buggey[4], G. Butcher[1,2], J. A. Carter[1], A. Cheney[1,2], H. Connor[18], T. Crawford[2], N. Eaton[13], C. Feldman[1,2], T. Frantzen[5], G. Galgóczi[21], J. Garcia[8], G. Y. Genov[5,15], H-P. Grőbelbauer[11], M. Guedel[6], Y, Guo[22], M. Hailey[3], D. Hall[4], R. Hampson[1,2], O. Hetherington[4], A. Holland[4], S-Y, Hsieh[17], M. W. J. Hubbard[4], H. Jeszenszky[7], M. Jones[1], T. Kennedy[3], K. Koch-Mehrin[1], S. Kőgl[12], S. Krucker[11], K. D. Kuntz[18], C. Lakin[1], G. Laky[7], O. Lylund[5], J. Miguel Mas Hesse[8], K. Oksavik[5], N. Østgaard[5], H. Ottacher[7], R. Ottensamer[6], C. Pagani[1], S. Parsons[4], P. Patel[2], J. Pearson[1,2], G. Peikert[14], F. S. Porter[18], T. Pouliantis[5], B. H. Qureshi[5], W. Raab[9], A. M. Read[1], N. M. M. Roque[5], M. E. Rostad[5], C. Runciman[9], S. Sachdev[2], A. Samsanov[3], D. Sibeck[18], S. Smit[3], J. Søndergaard[16], R. Speight[2], S. Stavland[16], M. Steller[7], T. Sun[10], J. Thornhill[1], W. Thomas[3], K. Ullaland[5], B. Walsh[19], D. Walton[3], C. Wang[10], S. Yang[5]

[1]School of Physics and Astronomy, University of Leicester, LE1 7RH, UK
[2]Space Park Leicester, University of Leicester, UK
[3]Mullard Space Science Laboratory, University College London, UK
[4]Centre for Electronic Imaging, Open University, UK
[5]Birkeland Centre for Space Science, University of Bergen, Norway
[6]University of Vienna, Austria
[7]Space Research Institute, University of Graz, Austria
[8]National Institute of Aerospace Technology, Spain
[9]ESTEC, European Space Agency
[10]State Key Laboratory of Space Weather, National Space Science Centre, China
[11]University of Applied Sciences and Arts Northwestern Switzerland, Switzerland
[12]Koegl Space GmbH, Switzerland
[13]Space Acoustics GmbH, Switzerland
[14]Zurich University of Applied Sciences, Switzerland
[15]Genov Solutions, Norway
[16]STM Engineering, Norway
[17]John Hopkins University Applied Physics Laboratory, USA
[18]NASA/Goddard Space Flight Centre, MD 20771, USA
[19]University of Boston, MA 02215, USA
[20]Department of Theoretical Physics and Astrophysics, Masaryk University, Czech Republic
[21]Institute of Physics, Eötvös Loránd University, Hungary
[22]Aerospace Information Research Institute, Chinese Academy of Sciences, China

Solar wind Magnetosphere Ionosphere Link Explorer: SMILE

SMILE is a collaborative science mission between

the European Space Agency (ESA)

and

the Chinese Academy of Sciences (CAS)

SMILE was one of 13 candidate mission proposals proposed by various groups for a joint mission AO. SMILE was selected by ESA and CAS in 2015 as the *winning* proposal.

With CAS funding, around x2 ESA Small Class budget (about ~1/3 ESA M Class budget)

SMILE Mission Adoption (ESA) in March 2019. Launch due in March 2025.

The Soft X-ray Imager (SXI) instrument on SMILE has just passed the checkpoint of the ESA iCDR and is entering the FM build stage.

SMILE Orbit and Primary Science Target

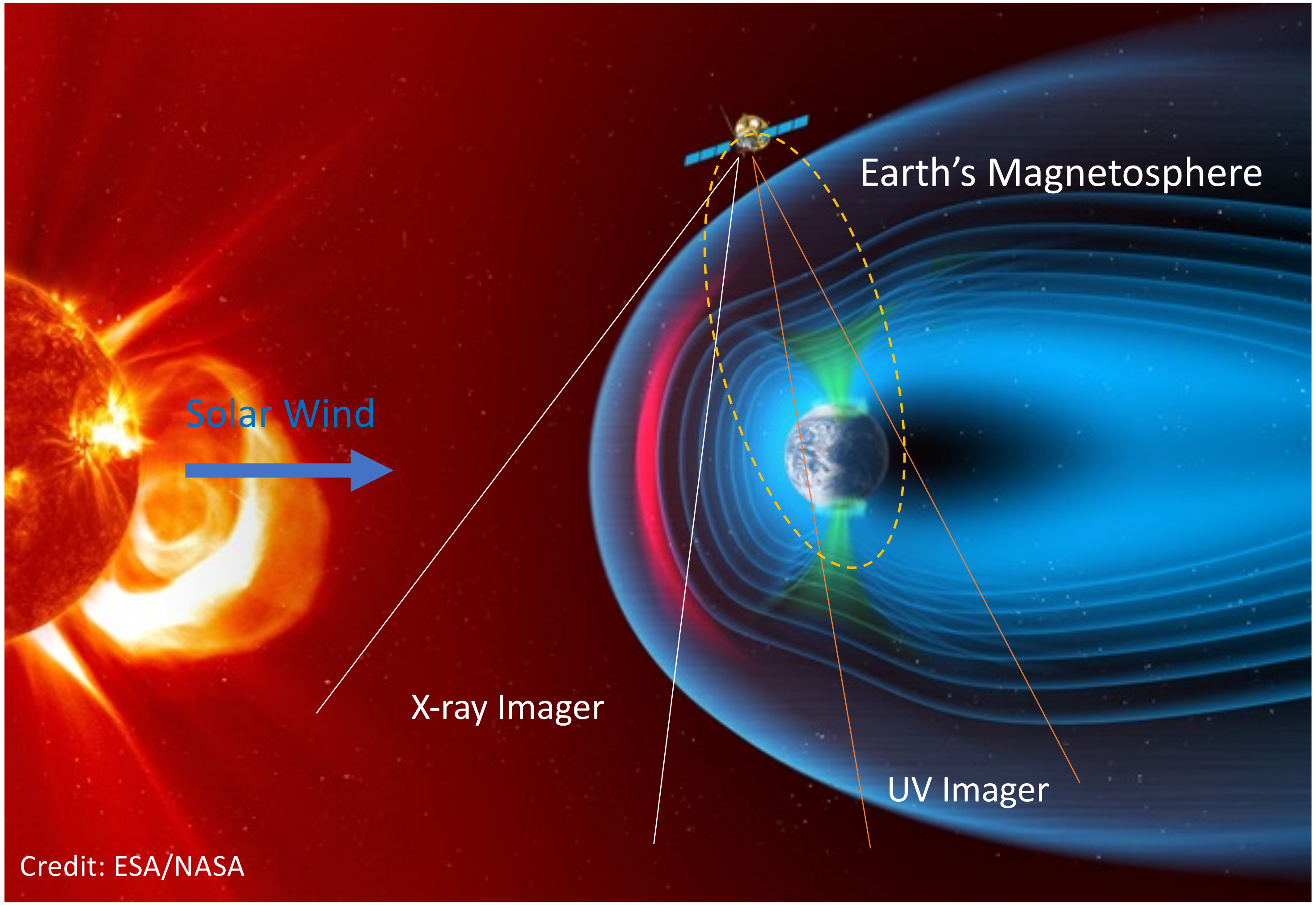

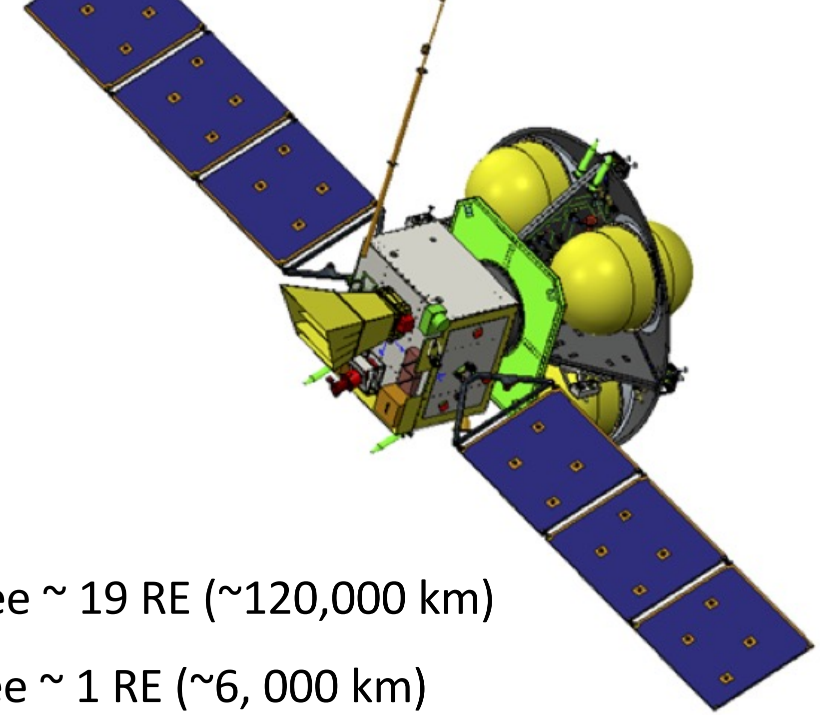

Orbit:

Apogee ~ 19 RE (~120,000 km)

Perigee ~ 1 RE (~6, 000 km)

Inclination: ~73°

Period: ~51 hours.

Science window: ~42 hours

Launcher: Vega-C

Nominal Mission Length = 3 Years

Maximum Mission Length ~ 7 Years

Global imaging using Solar Wind Charge Exchange (SWCX)

SWCX: High charge state solar wind ions in collision with hydrogen in the Earth's exosphere to produce photons at X-ray energies

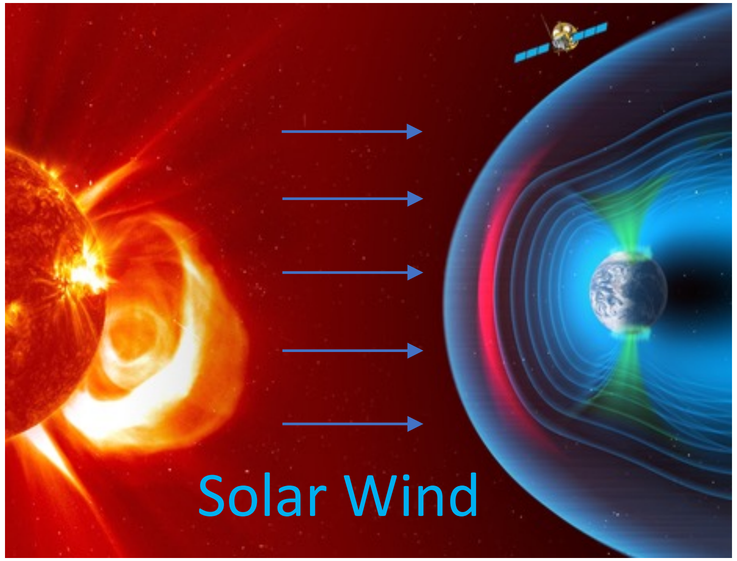

Solar Wind: electrons & protons with some (~2%) heavy ions such as carbon, nitrogen and oxygen embedded in the Sun's magnetic field

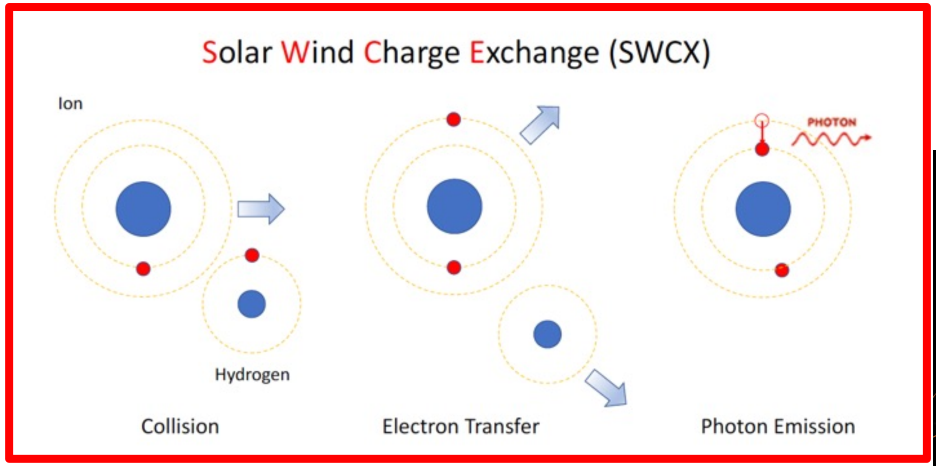

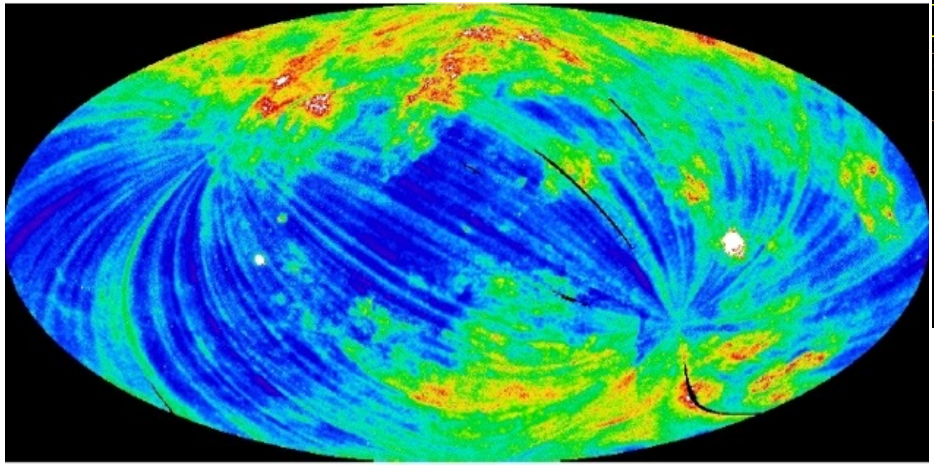

ROSAT All-Sky Survey in 1990 (Scanning observations)
SWCX Can be brighter than X-ray background

No Solar Wind in these regions therefore no SWCX X-rays

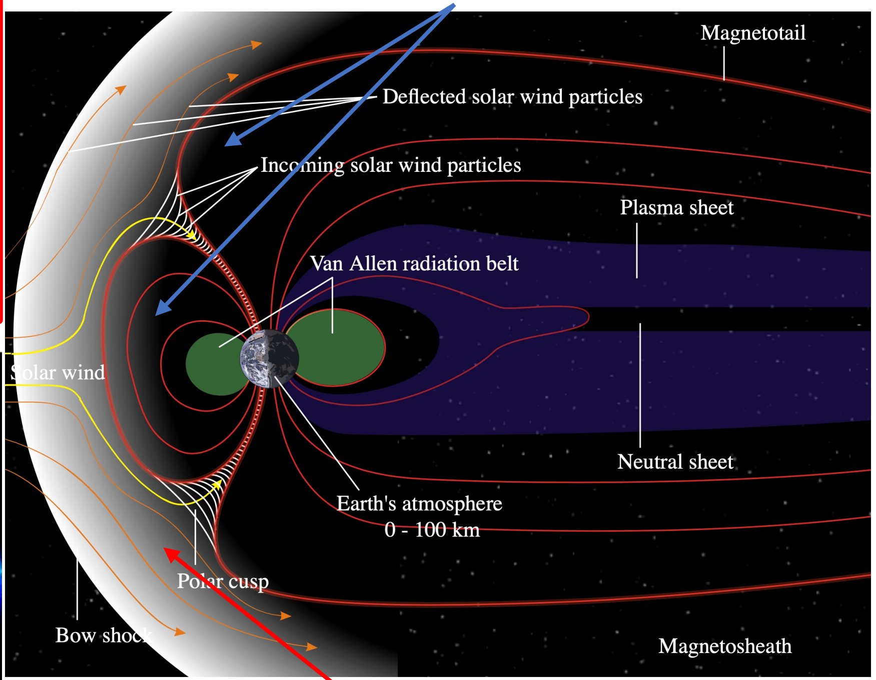

Solar Wind in these regions therefore SWCX X-rays

Hence: magnetopause boundary can be detected using X-ray imaging

SMILE Instruments and Spacecraft

Soft X-ray Imager (SXI)
PI: Steve Sembay (Uni. Leicester, UK)

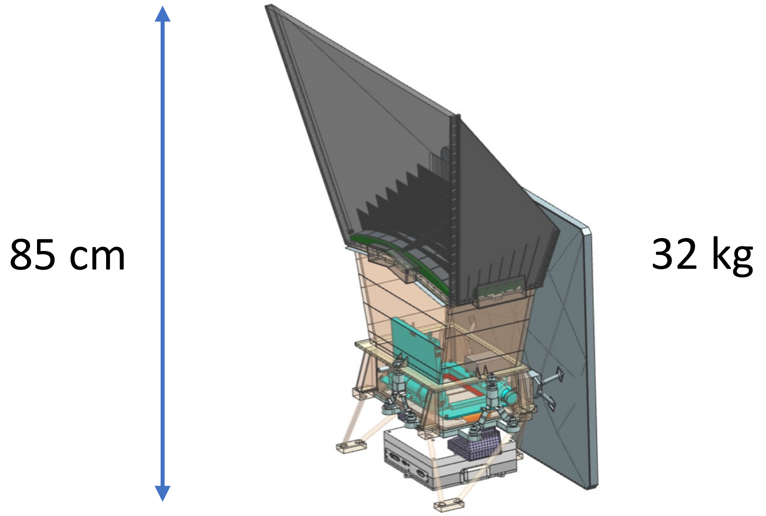

Ultraviolet Imager (UVI)
PI: X. Zhang (NSSC, China)

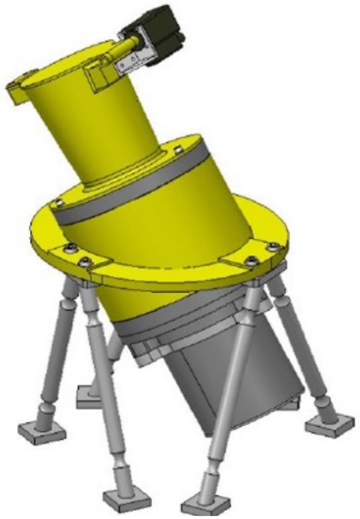

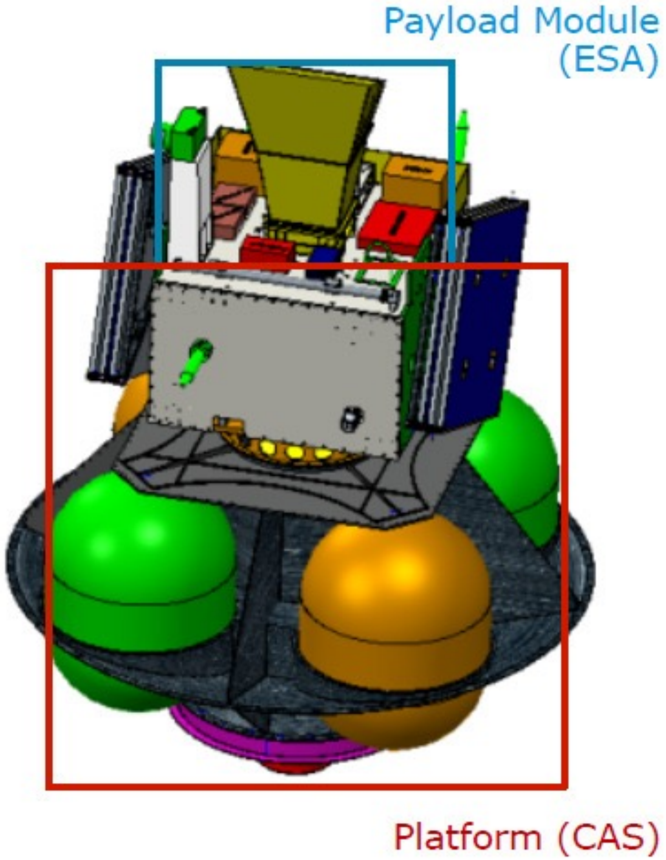

Light Ion Analyser (LIA)
PI: Lei Dai (NSSC, China)

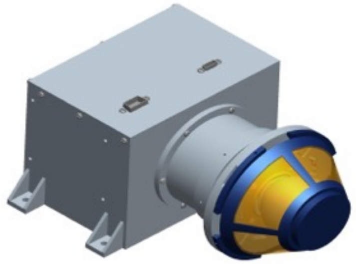

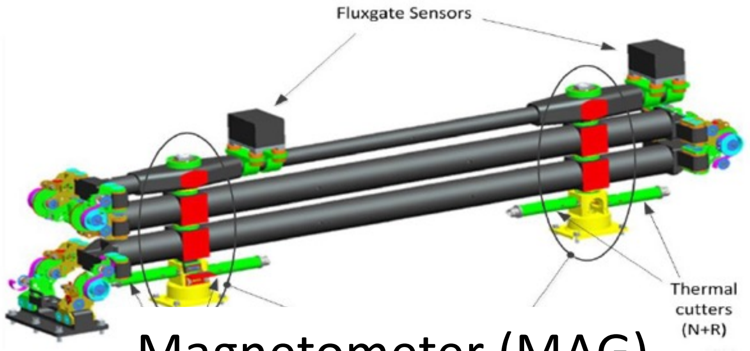

Magnetometer (MAG)
PI: Lei Li (NSSC, China)

Launched by ESA on Vega-C
Operations responsibility is CAS

NSSC: National Space Sciences Centre, Beijing (http://english.nssc.cas.cn)

SMILE Ground Segment Architecture

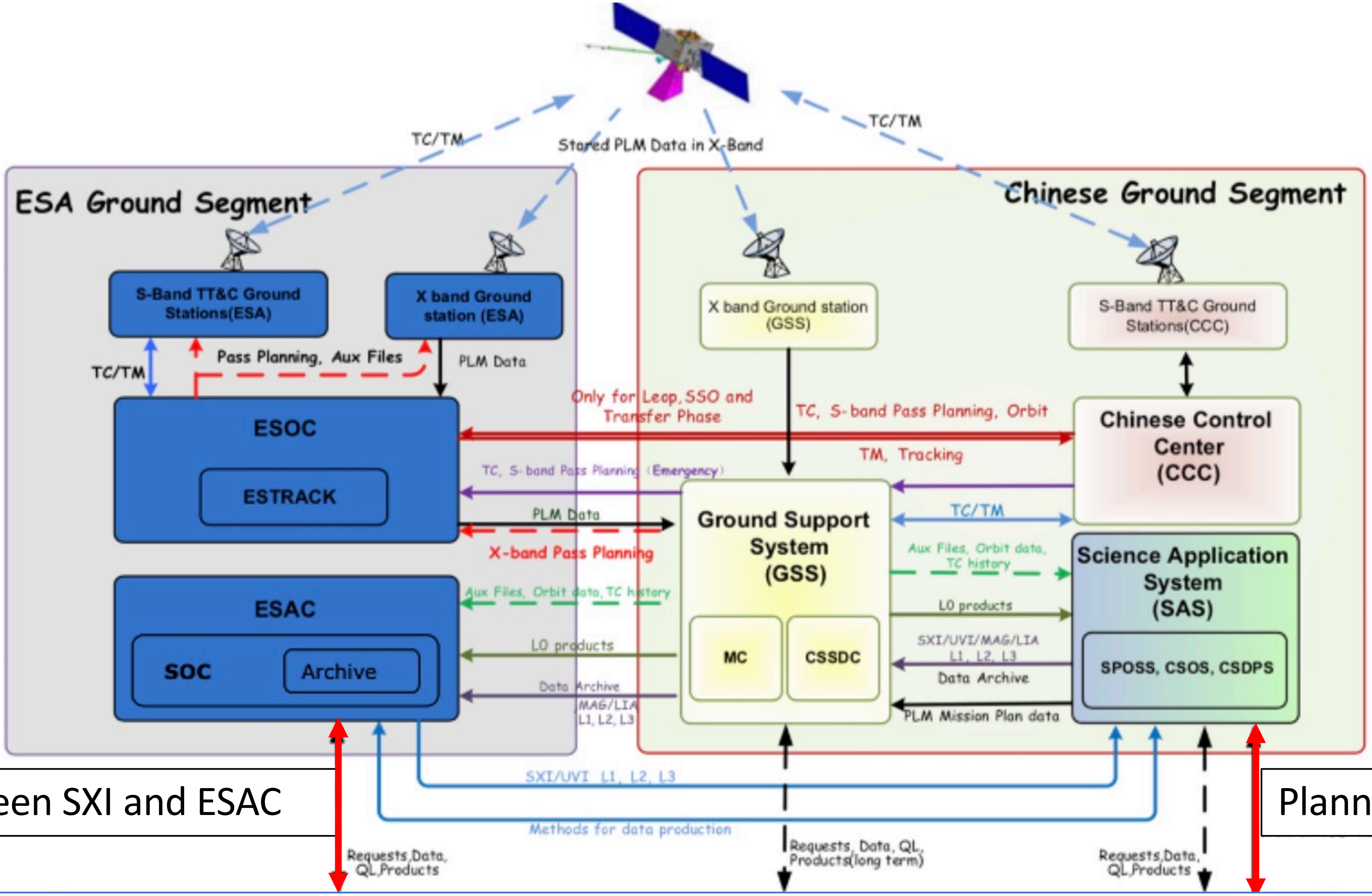

Data flow between SXI and ESAC

Planning Interface with PI

SXI CONSORTIUM

Responsible for Instrument Planning and Data Processing to Archive

SXI: Soft X-ray Imager Hardware (Height ~ 85cm, Mass ~ 32 kg)

University of Leicester (PI)

UCL Mullard Space Science Laboratory

The Open University

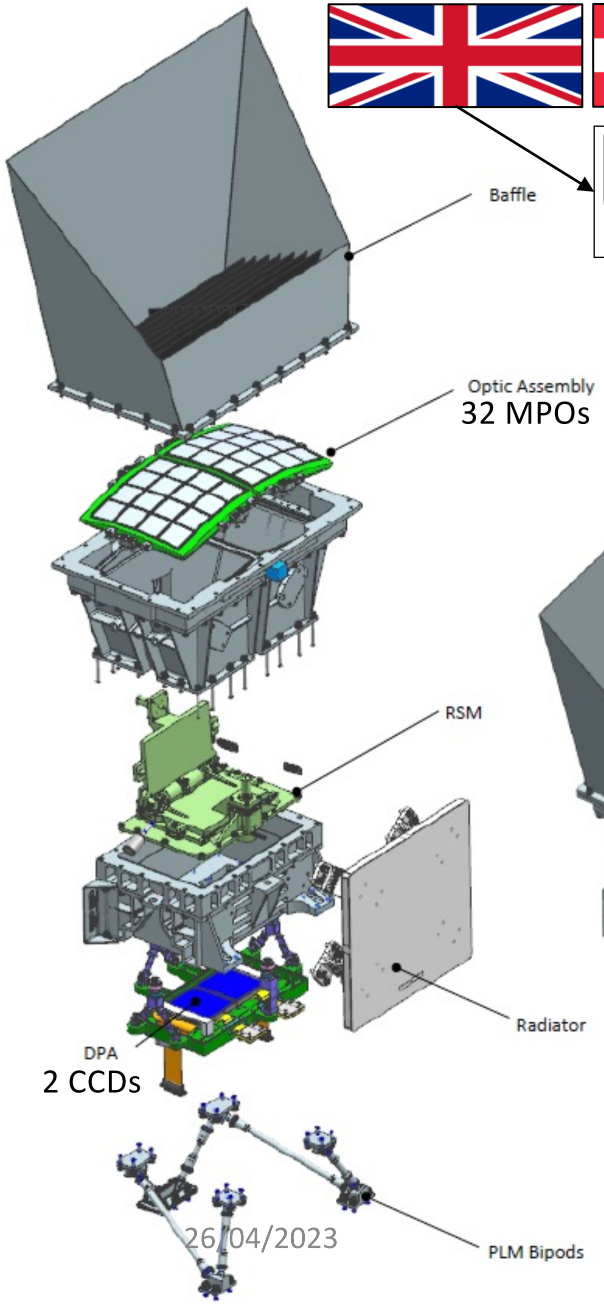

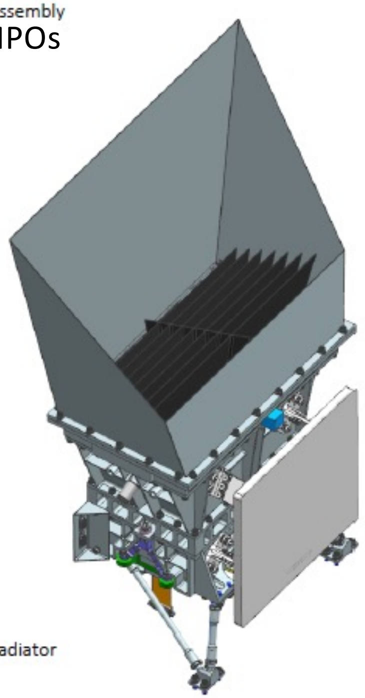

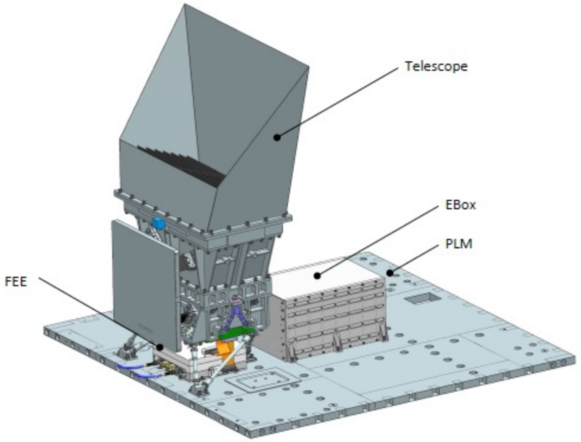

Key Technology:
Large Area X-ray sensitive CCDs; developed by Te2v, UK

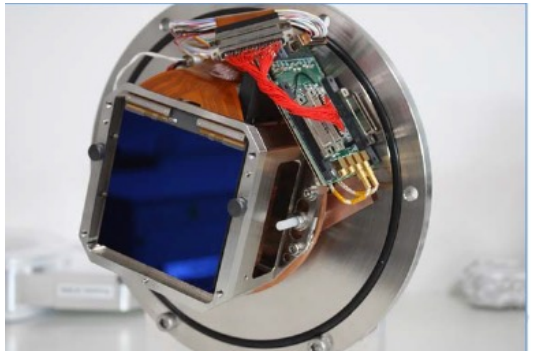

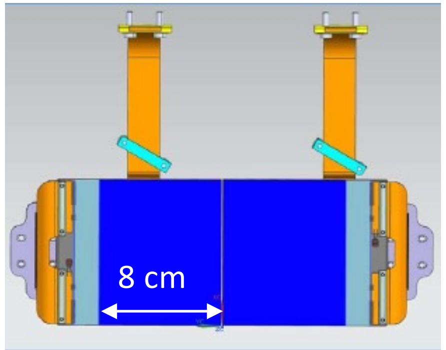

Key Technology:
Micropore Optics (MPOs); developed by Photonis SAS, France in collaboration with UoL

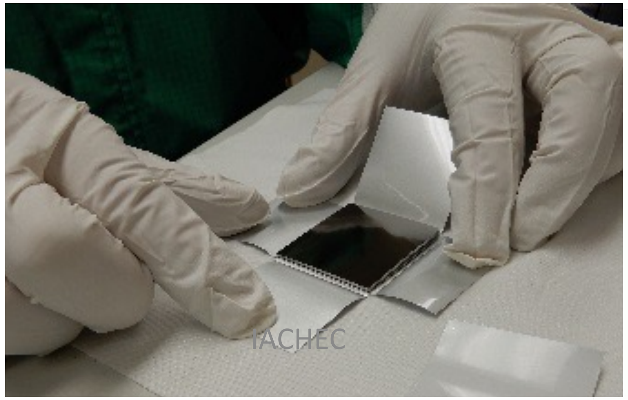

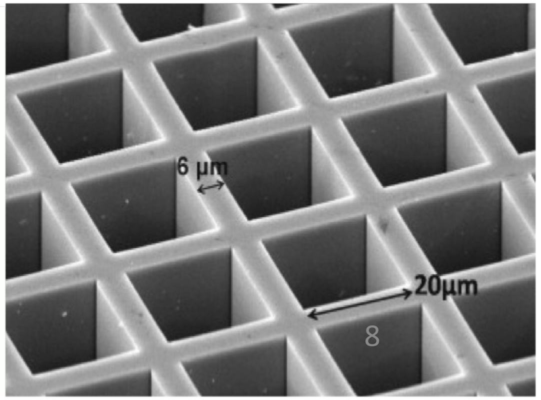

Optic Assembly: Lobster-Eye Configuration

32 MPOs in two 4 x 4 Assemblies

MPOs are 4 cm x 4 cm, 1.2 mm thick

40 micron channels with 12 micron wall thickness

Iridium coated channels

100 nm Aluminium optical filter on top

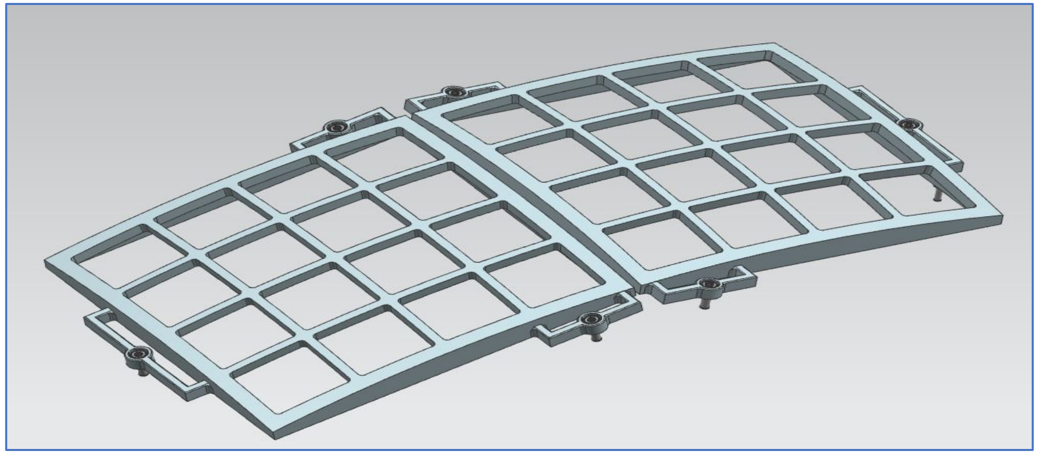

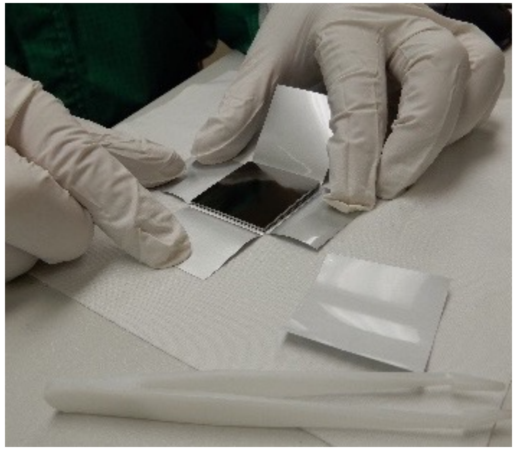

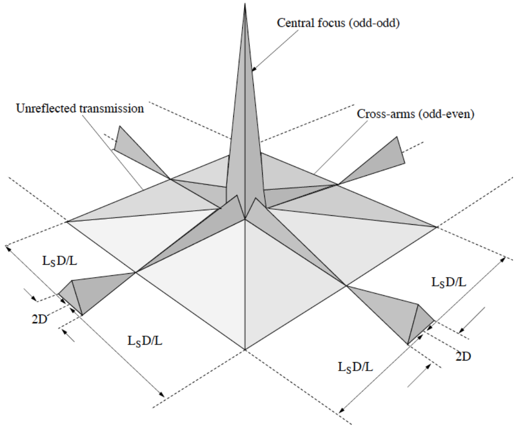

Detector Assembly: X-ray sensitive CCDs

Two Te2V CCD 370 devices (derived from PLATO CCD270)

Back-illuminated, 18 micron depletion depth

8.11 x 8.11 cm with 4510x4510 18 micron native pixels

Anti-reflective coating removed

Supplementary Buried Channel (SBC) to improve CTI

X-ray detection mode: 6x6 binning with asymmetric frame store

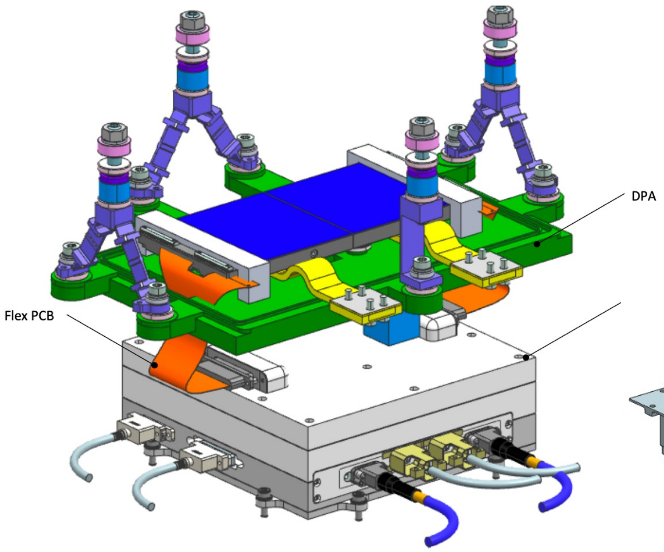

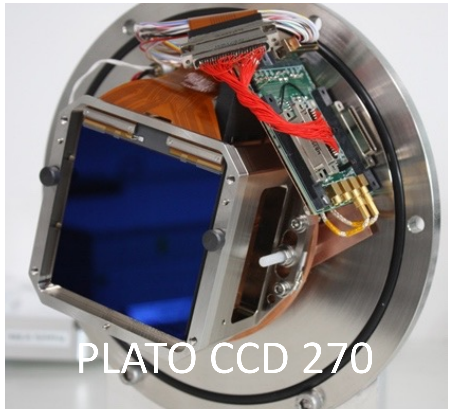

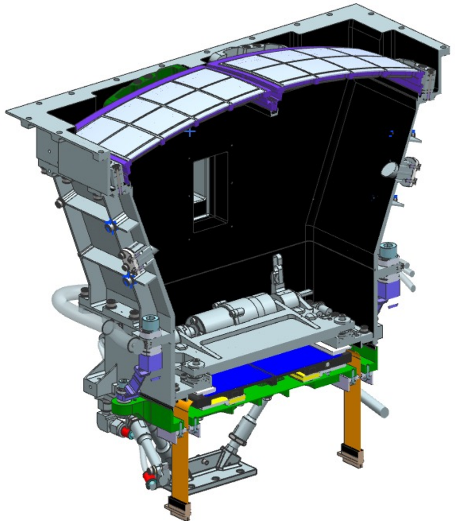

SXI STM at RALSpace Undergoing Vibration Test (April 2021)

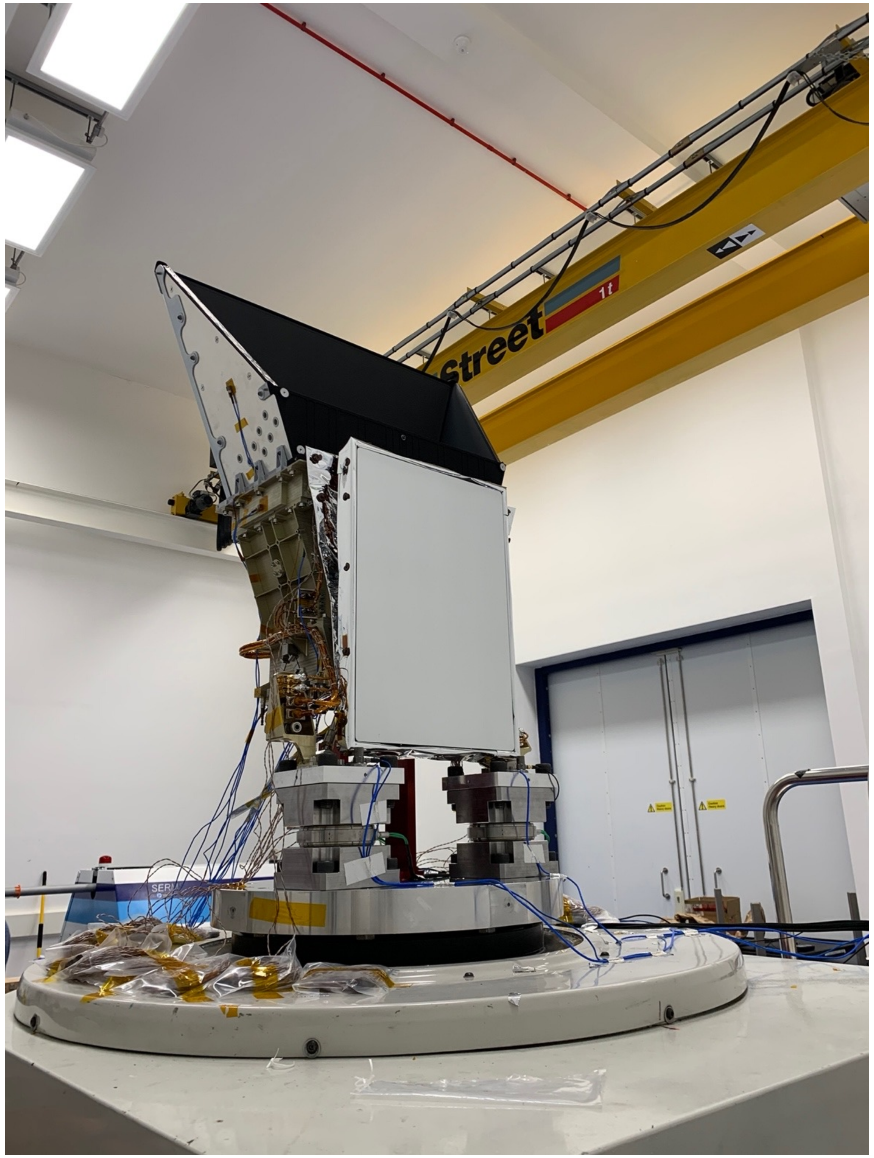

SXI STM (centre) and UVI STM (left) mounted on PLM at Airbus, Spain.

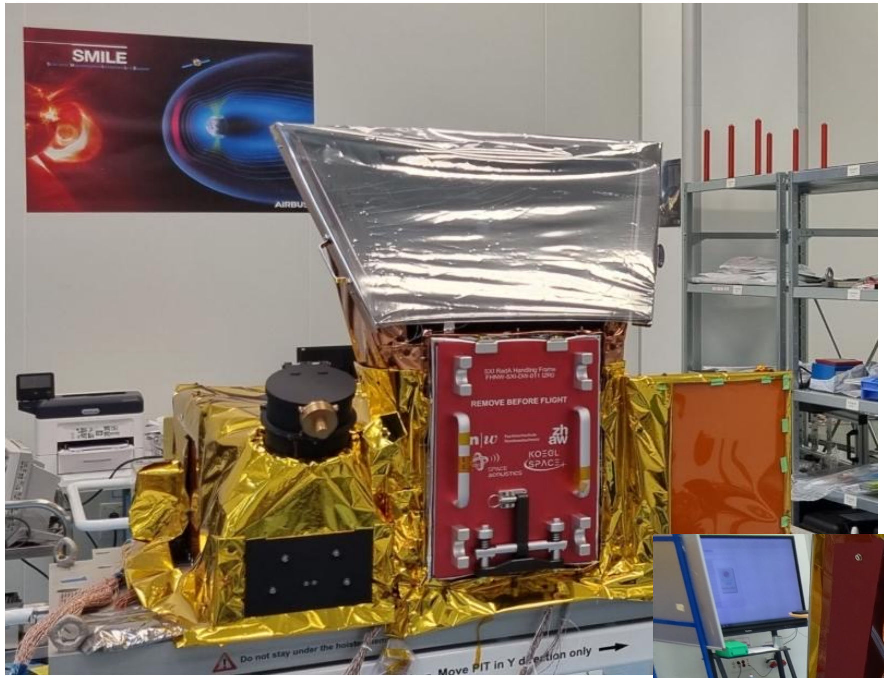

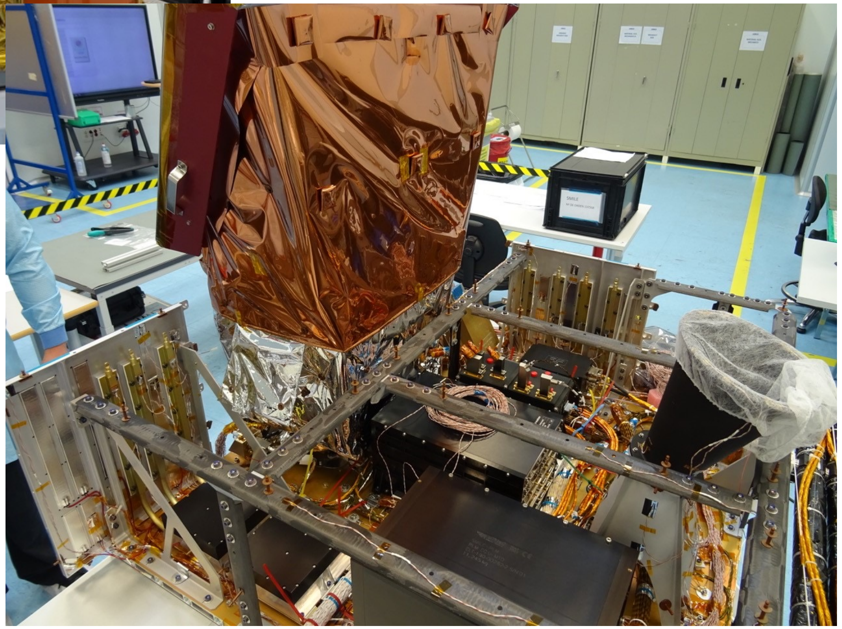

SXI Instrument simulations from MHD (PPMLR) input

SXI delivers time-tagged photon lists which are reconstructed on-ground into images and spectra.

Medium Solar Wind
Flux = 4.9×10^{8} cm^{-2} s^{-1}

CTS Image:
Exposure = 300s
Pixels = 1.0° x 1.5°

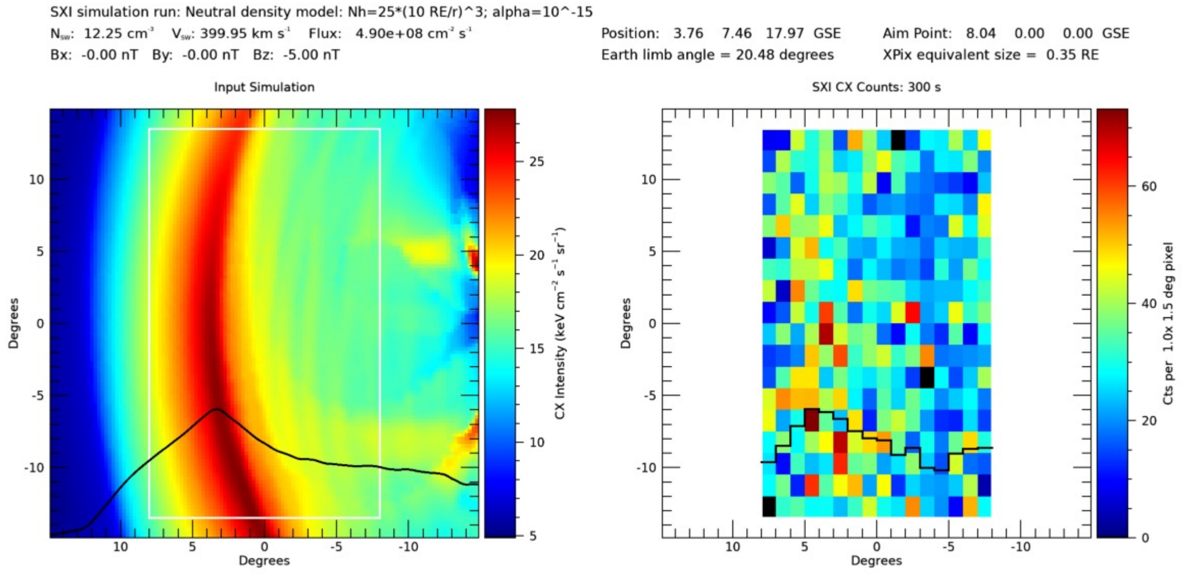

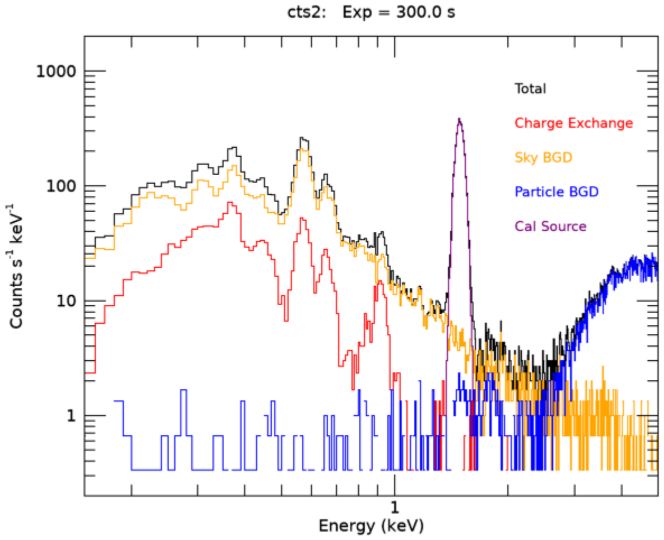

Strong Solar Wind
Flux = 1×10^{9} cm^{-2} s^{-1}

CTS Image:
Exposure = 300s
Pixels = 0.5° x 0.5°

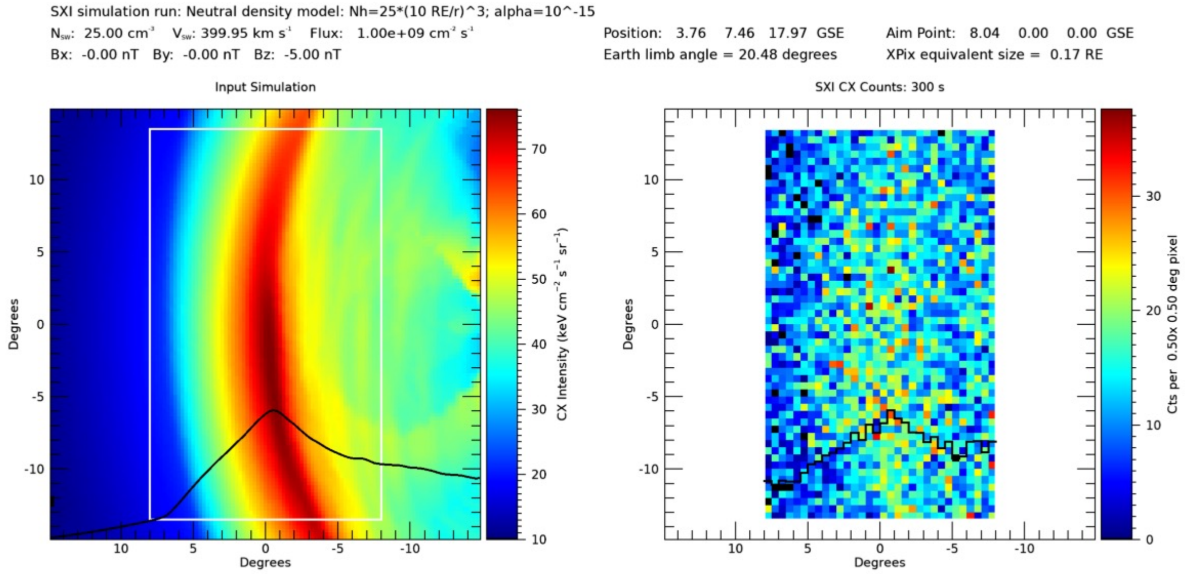

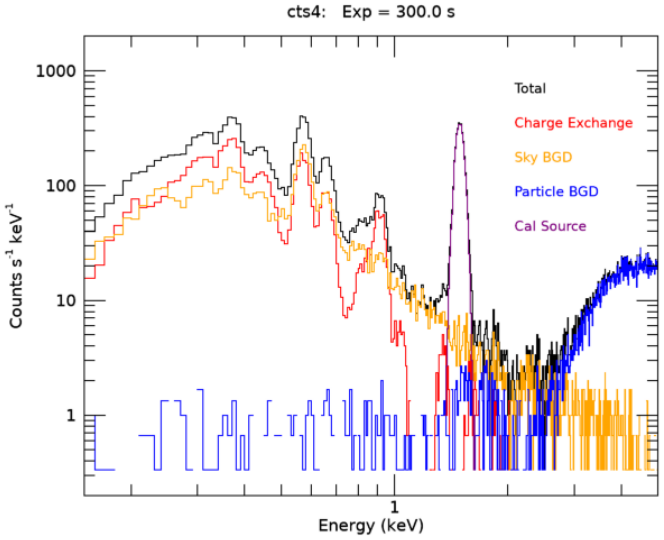

Data analysis challenges for SXI

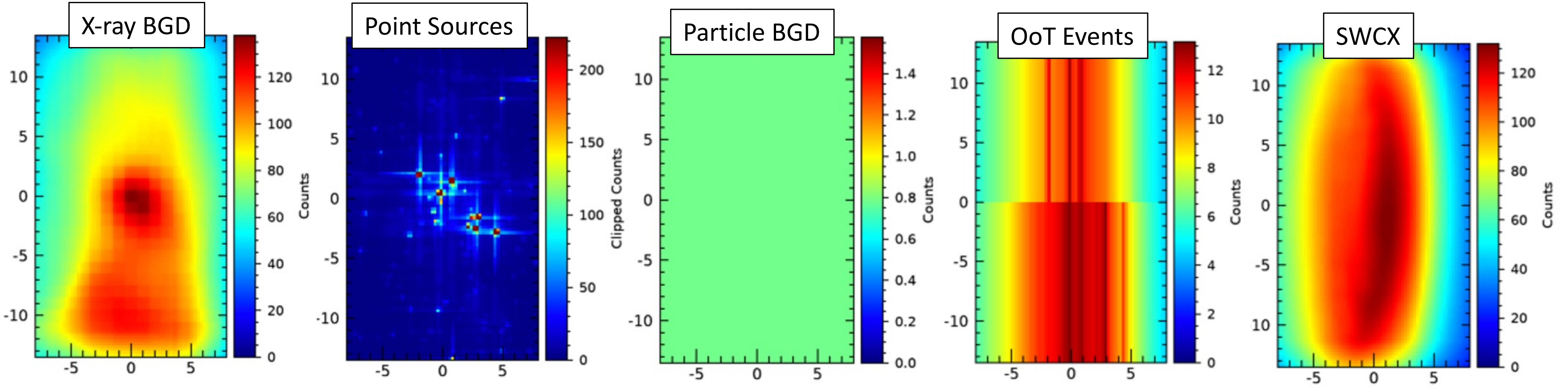

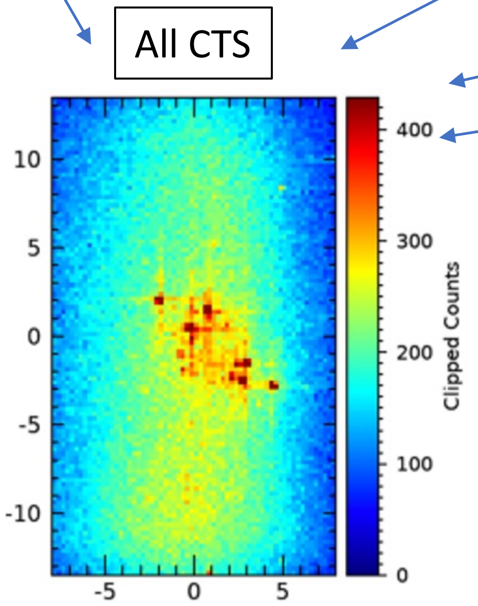

Background is not "easily" separable in SMILE SXI data

Going from this

to a magnetopause boundary ($R0_{MP}$) is not trivial

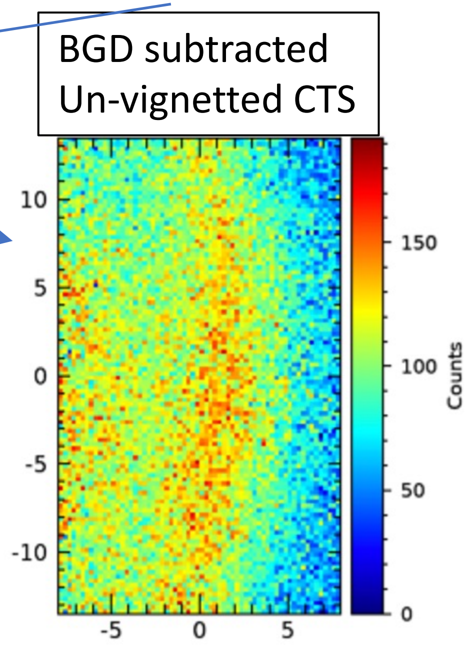

Reconstructing the Magnetopause Boundary; One Proposed Method

Forward Modelling using an empirical model of X-ray emissivity in the magnetosheath

From Jorgensen et al. 2019 JGR, 124, 6, 4365-4383

$$r_y(\theta) = r_0 \left(\frac{2}{1+\cos\theta} \right)^{\alpha_y}$$

$$r_z(\theta) = r_0 \left(\frac{2}{1+\cos\theta} \right)^{\alpha_z}$$

$$r(\theta,\phi) = \frac{r_y(\theta)\, r_z(\theta)}{\sqrt{[r_z(\theta)\cos\phi]^2 + [r_y(\theta)\sin\phi]^2}}$$

Theta – angle to GSE-X axis
Phi – angle around GSE-X axis

X-ray Emissivity

$$F(\vec{r}) = \begin{cases} 0 & \text{inside MP} \\ (A_1 + B\sin^8\theta)\left(\frac{r}{r_{ref}}\right)^{-(\alpha+\beta\sin^2\theta)} & \text{between MP and BS} \\ A_2\left(\frac{r}{r_{ref}}\right)^{-3} & \text{outside BS} \end{cases}$$

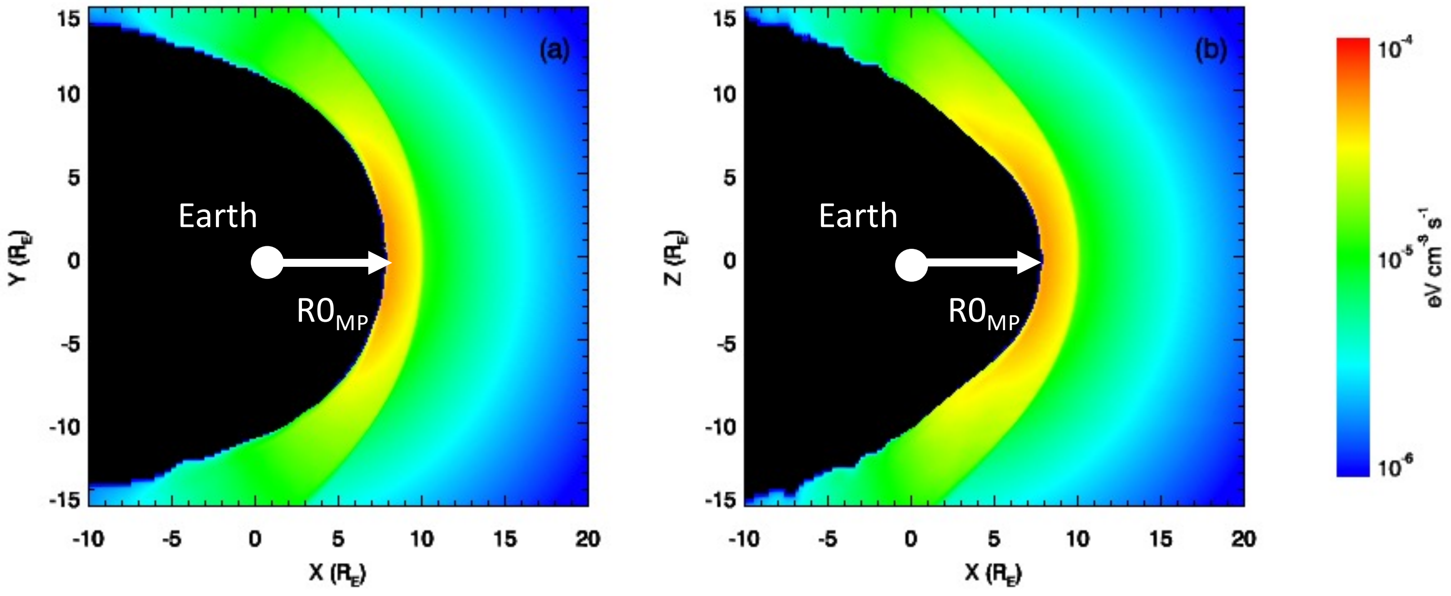

Reconstructing the Magnetopause Boundary: Best fit parameters found by Chi-squared Minimisation

MHD + SWCX assumptions used to derive predicted 3D X-ray emissivity cube from which 2D Map for a given spacecraft position and look direction is derived.

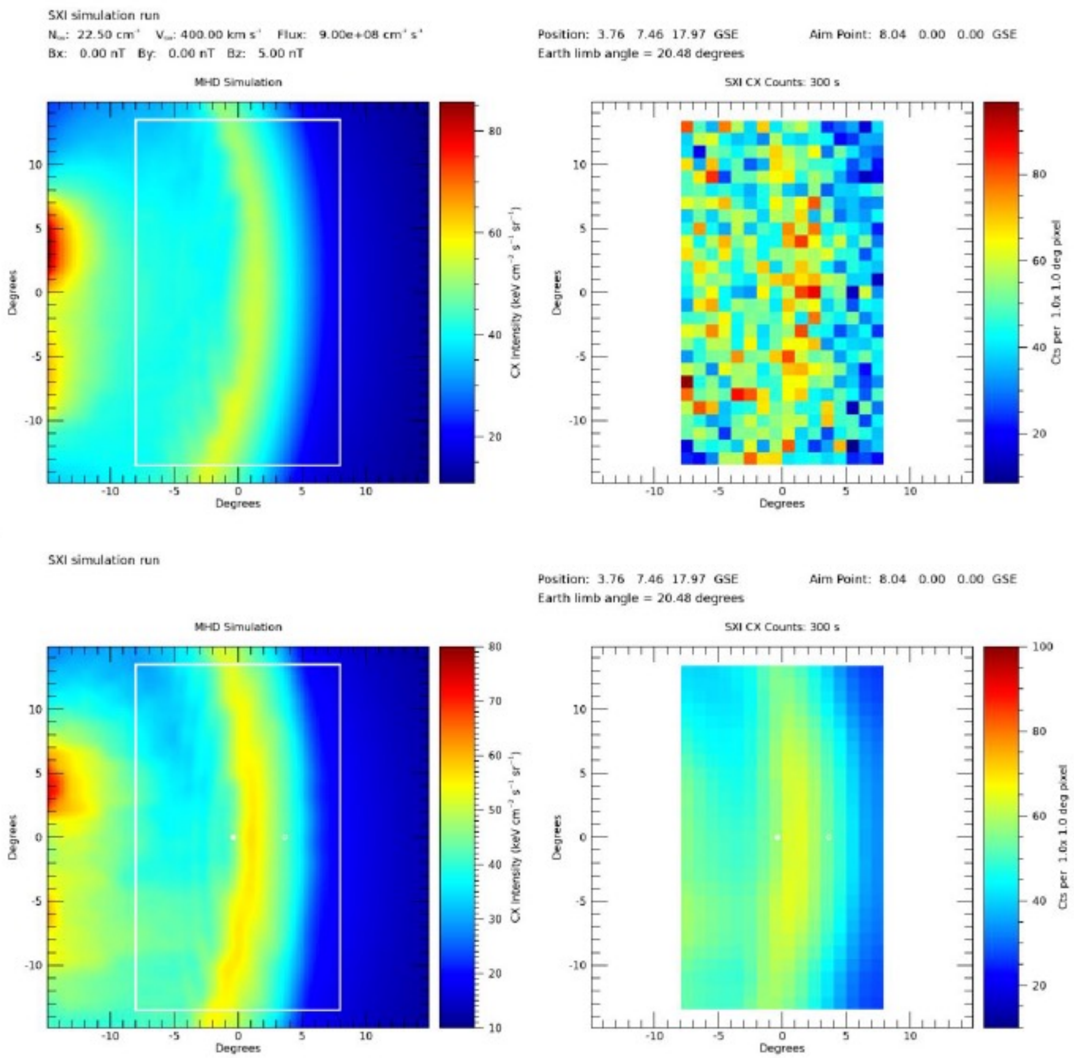

sxi_sim output with noise

-> Dataset

Minimise Chi-squared to find best fit parameters

-> Model

sxi_sim output Without noise

Parameterised empirical model used to derive predicted 3D cube from which 2D Map for same spacecraft position is also derived.

Model has $R0_{MP}$ & $R0_{BS}$ plus loads of other parameters

Reconstructing the Magnetopause Boundary: Estimated error on $R0_{MP}$

- Mean Error in $R0_{MP}$ for 5 minute exposure

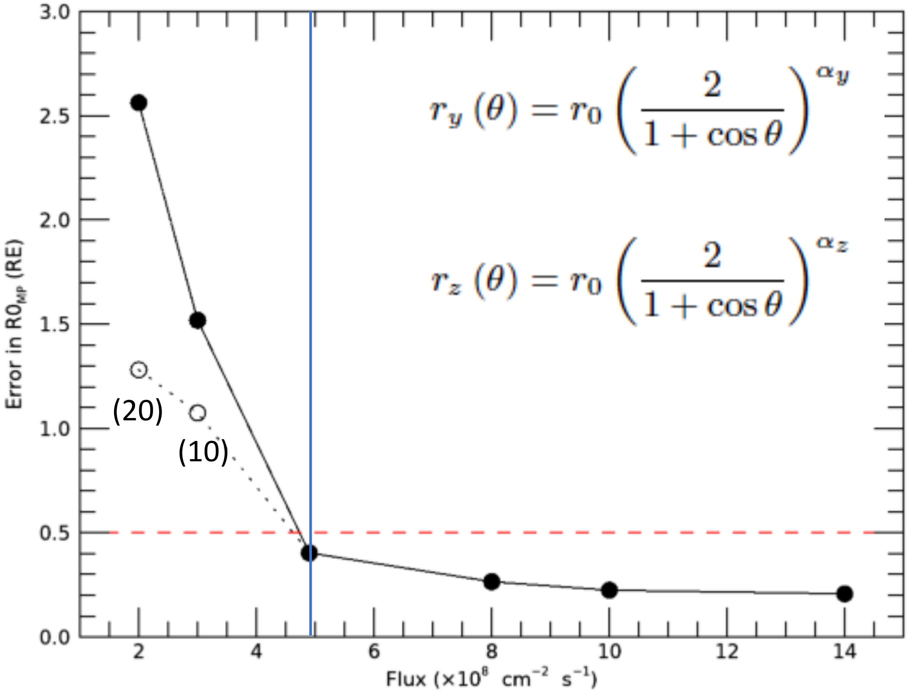

Forward Modelling

Pros:

1) Requires one image (due to FOV some portion of orbit better than others)

2) Simpler way to handle instrument response

Cons:

1) More assumptions: Method only as good as the underlying empirical model

2) Computationally intensive

Position of subsolar magnetopause position derivable to better than 0.5 RE in 5 minutes for solar wind fluxes >~ 5×10^{8} cm^{-2} s^{-1}

Example of estimating calibration sensitivity requirements: Vignetting function

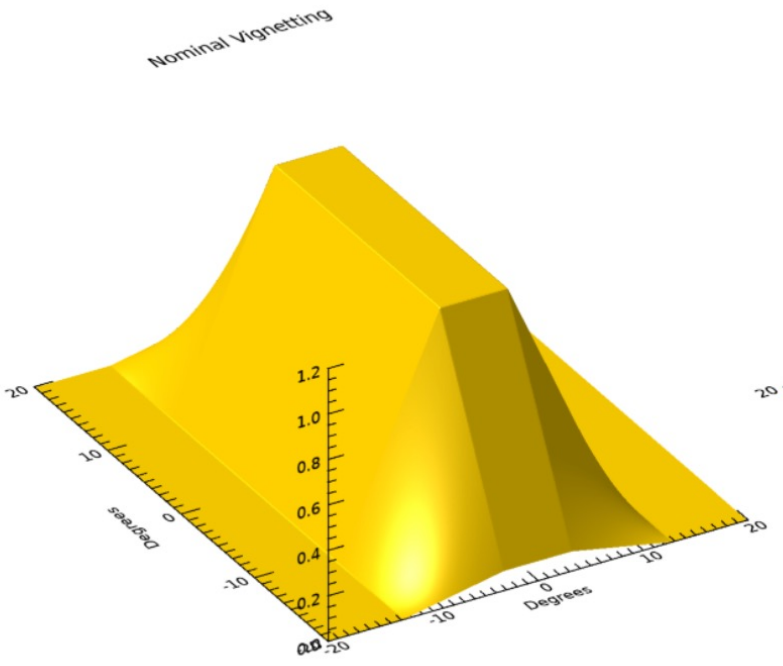

Ideal Vignetting Function

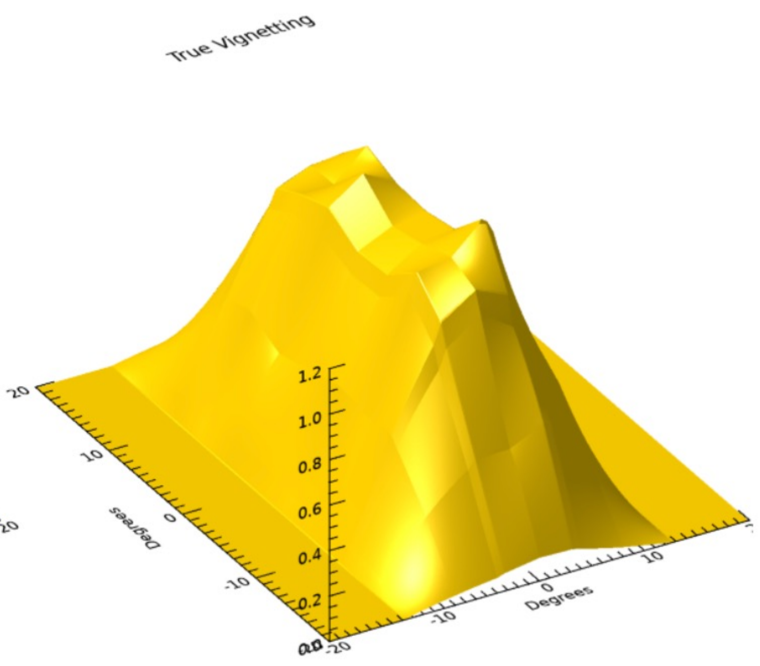

Vignetting Function modified randomly at nodal points

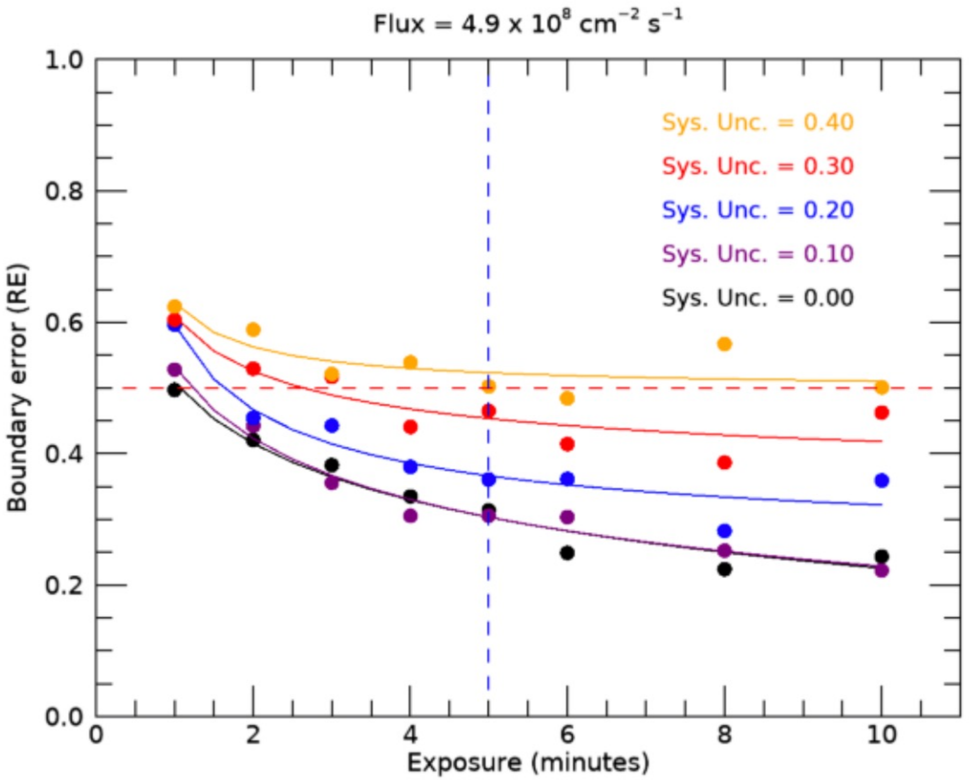

- Generate simulation with modified Vignetting function (and/or other instrument characteristics)
- Perform parameter estimate analysis assuming ideal function.
- Rinse and repeat many times to derive variance in derived parameters of interest

SMILE SXI Ground Calibration Overview (to date)

"*Ground calibration plans often have compromises*": Paraphrase of the calibration lessons learned talks by myself and D. Jerius at Woods Hole IACHEC 2010

Compromises in the SMILE SXI calibration programme from an absolute "gold standard" are due to the requirement of meeting the mission schedule and minimizing risk to FM components (there is no full FS instrument).

1. CCD QE and RMF data over science band taken at Bessy Synchrotron on QM CCD, not on final FM CCDs. FMs are comprehensively *characterized* (at Open University, next slide) but at limited energies compared with the QM. No significant mechanical differences between the two.

2. Optics calibration for FM will be at the individual frame level (at UL), not on the whole sub-assembly level (typically done at the Panter due to its larger chamber).

3. No full instrument end-to-end calibration planned. This is because the radiation shutter mechanism (RSM) has a once-operated launch lock pin which can only be primed on the bench. This means RSM has to be installed with door covering the detector plane.

Despite this, we will have sufficient confidence in the performance of the instrument from ground data but it adds emphasis to the importance of in-flight calibration …. See Andy's talk.

CCD Calibration and Characterisation by team at Open University:

The characterisation includes an assessment of:

- Noise
- Energy resolution
- Dark Current
- Bright defects
- Assessment of the charge injection structure uniformity
- Trap Pumping for defect identification
- X-ray CTI with an Fe55 source
- EPER CTI over a range of charge levels
- Quantum efficiency between 50eV – 1900 eV

QE and RMF ground calibration measurements (Bessy Synchrotron) of QM CCD.

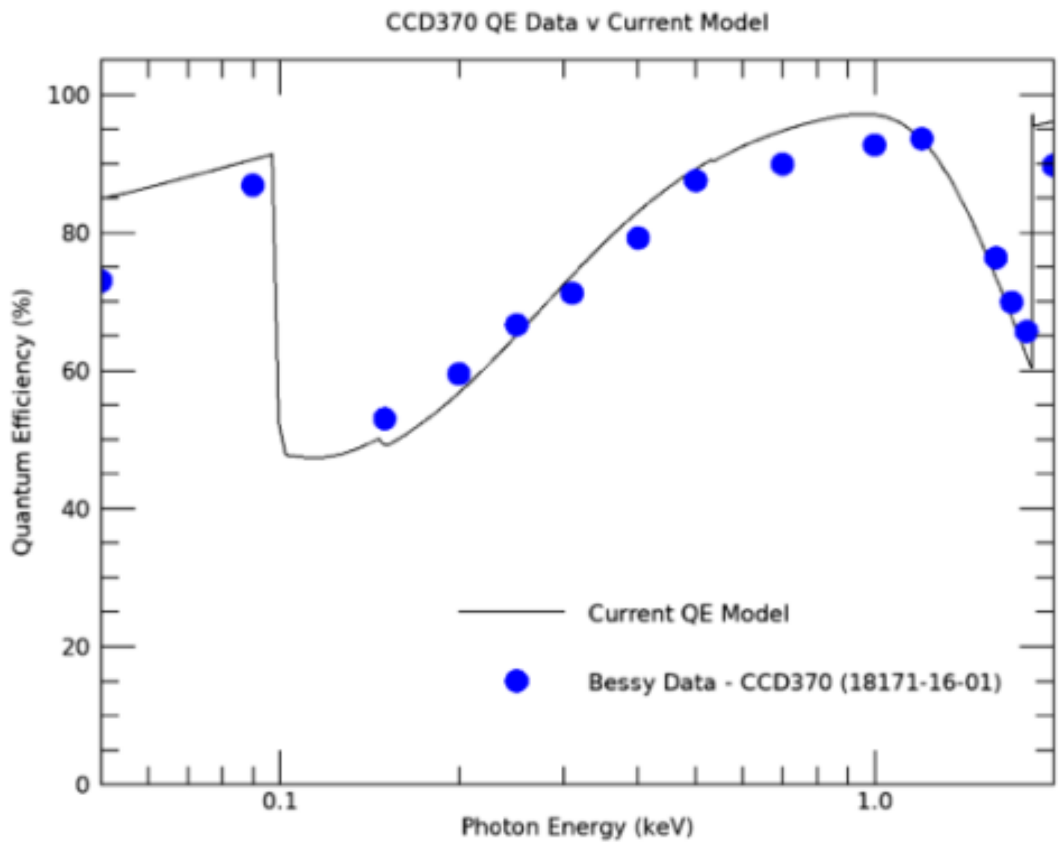

Data Source: Open University, UK

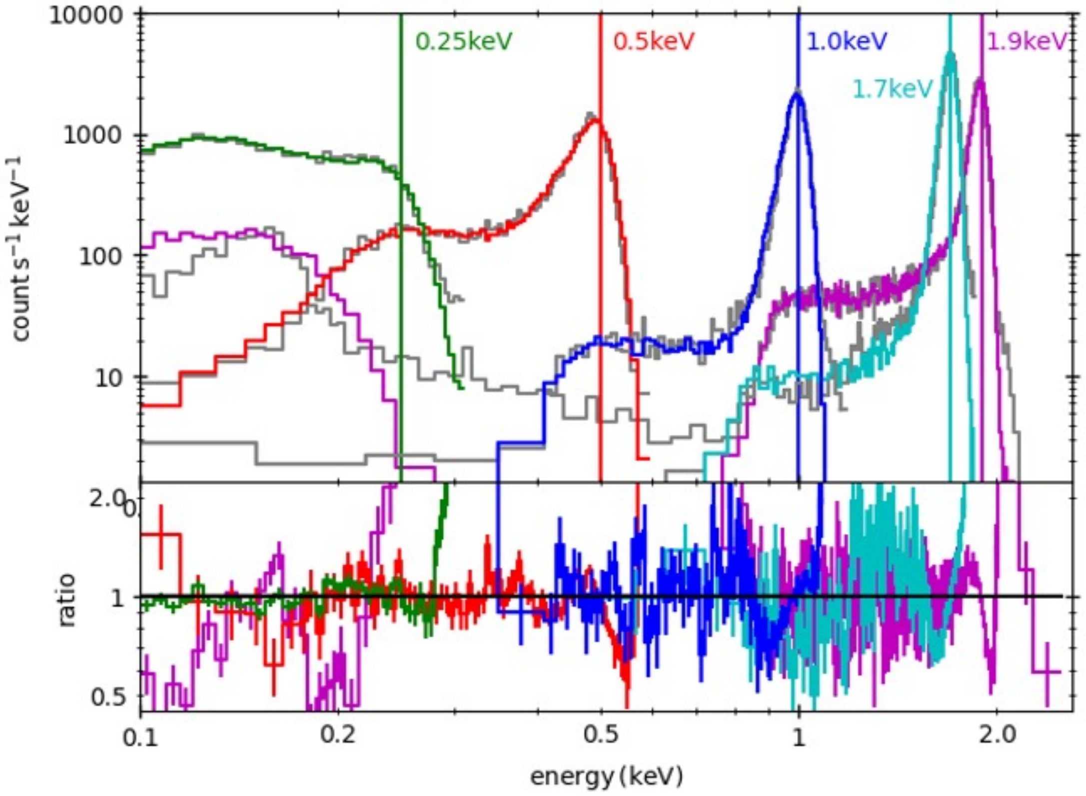

RMF Model fit to Data from Andy Beardmore (UL) CCD model

SXI Optical Arrray:

- Two 4x4 MPO assemblies (32 MPOs total)
- 600 mm (specified) radius of curvature, 300 mm focal length
- 40 micron wide channels of 1.2 mm length giving 1:30 width to length ratio: Optimises throughput over angular resolution.
- Covered by 100 nm Aluminium film for straylight suppression.

QM MPO measurements

Plate	ROC (mm)	C-K (277 eV) FWHM, X & Z (')		Cu-L (929 eV) FWHM, X & Z (')	
AG000-B1	586	11.15	12.06	10.43	10.99
AG001-B3	578	16.01	12.27	13.20	10.93
AG001-B5	578	11.31	12.62	10.87	12.09
AG001-B8	585	12.04	14.13	11.93	14.13
AG001-B9	585	11.30	11.45	10.66	11.24
AG001-B11	576	13.31	12.94	13.23	12.93
AG001-B13	544	28.01	27.48	31.57	29.82
AG001-B14	575	17.46	16.02	17.32	16.87

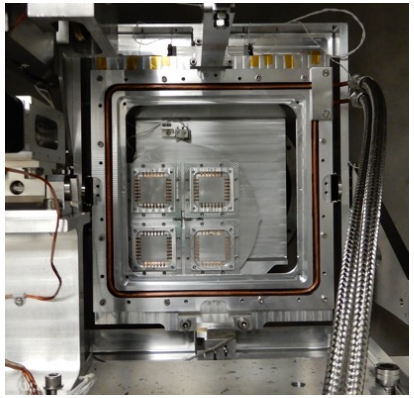

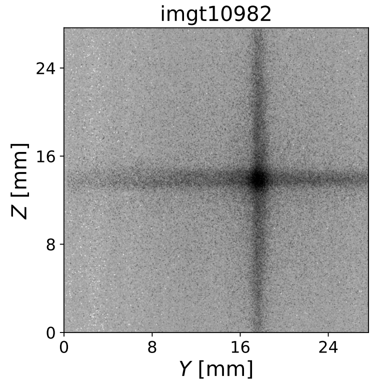

Mean ROC = 580mm +/-4.4 mm (excluding B13)

PSF (Core) FWHM in 11' to 13' range

Influence of PSF

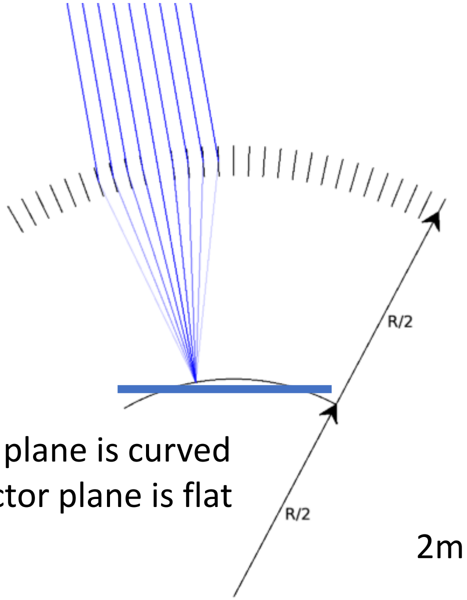

Focal plane is curved
Detector plane is flat

2mm Offset

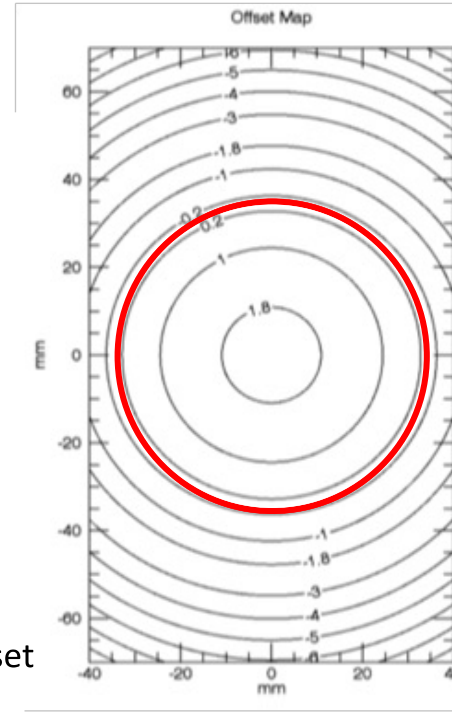

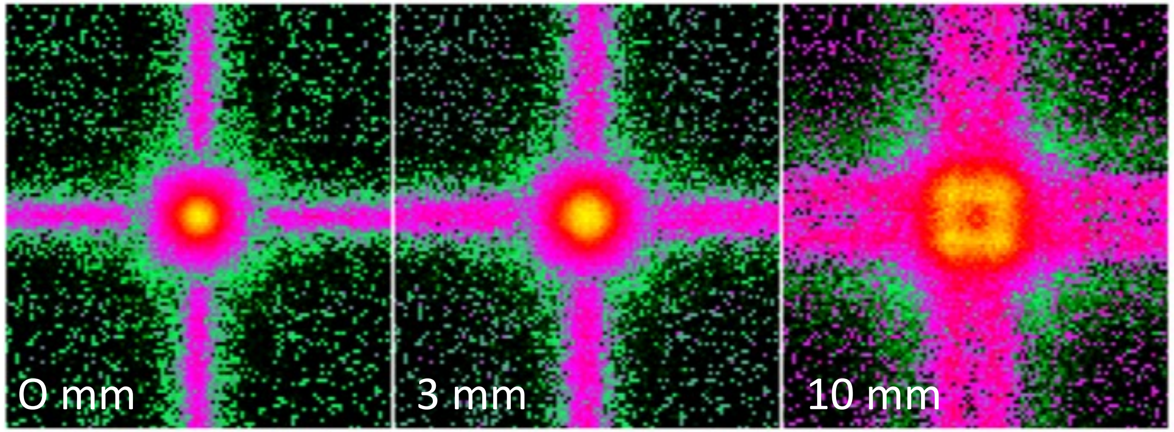

Figure 4: Zoomed PSF assuming detector to focal plane offsets of 0 mm (left panel), 3 mm (middle panel) and 10 mm (right panel) respectively.

~ x 3 broadening of PSF

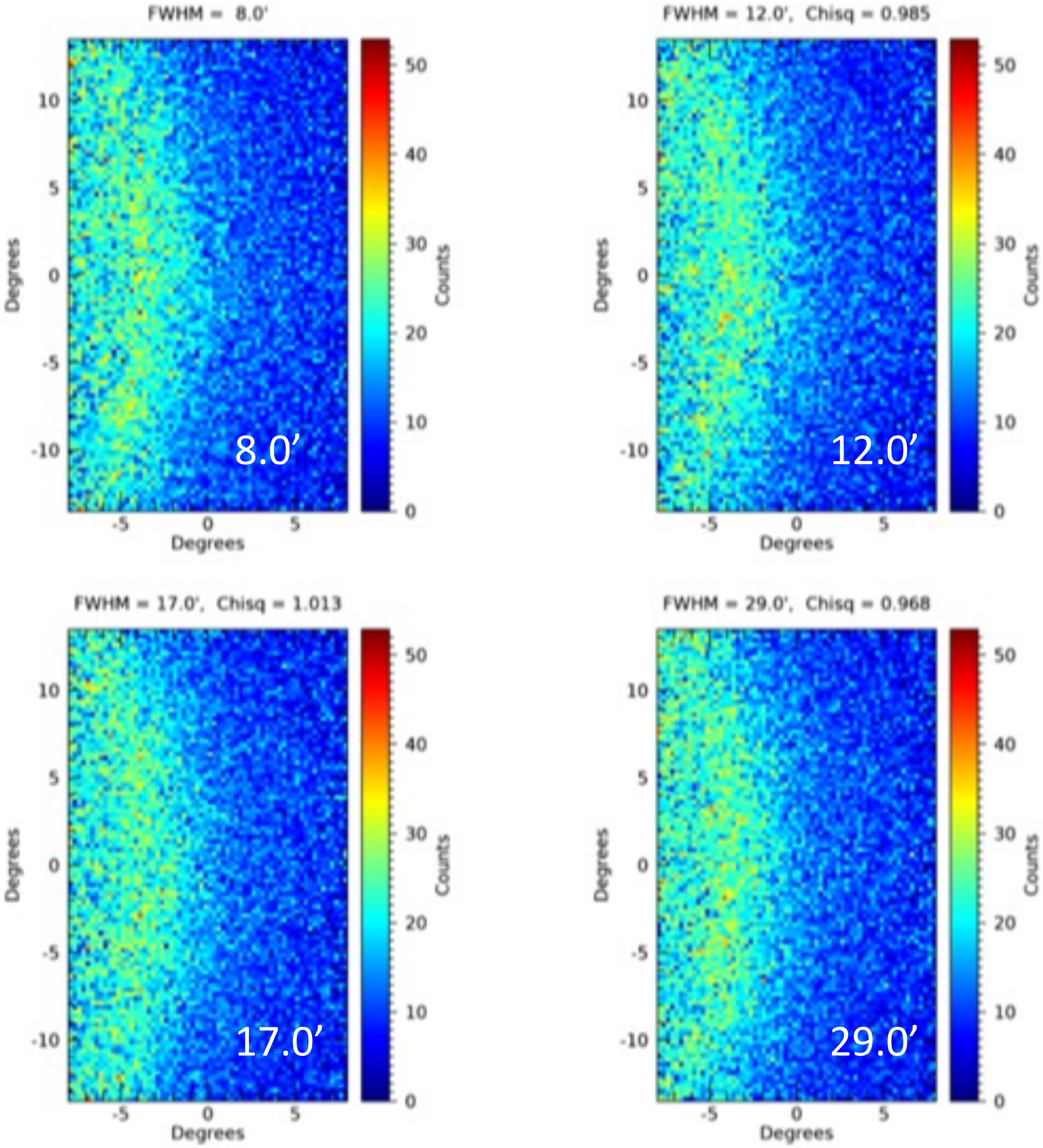

Figure 31: Four SXI simulations (exposure = 1200 s, pixel = 15 arcminutes) with the same solar wind input (flux = $1.4x10^9$ *cm-2 s-1) varying only by the FWHM of the PSF as shown. The reduced chi-squared difference between the first and second to fourth images is 0.985, 1.013 and 0.968 for 6911 DOF.*

SMILE SXI Performance Figures

Parameter	Value (at 0.5 keV if relevant)	Comment
Optic focal length	290 mm	Measured (300 mm specified).
MPO pore size	40 µm	
MPO pore length	1.2 mm	L/D = 30:1
Optic coating	Iridium	
PSF FWHM	~ 11 to 15 arcminutes	Across 60% of the detector plane. In part due to the flat detector plane relative to the curved optical focal plane.
PSF HEW	~2.8 degrees	
Optic total effective area	14.6 cm^2	At centre of FOV
Optic FOV	32.1° x 15.8°	
Straylight baffle vignetting	~0.88	Min to max ranges by around +/- 0.06
CCD QE	0.89	
CCD energy resolution	50 eV (FWHM)	Assuming 4.5 e^- noise, BOL CTI
CCD frame integration time	5-10 Seconds	
Filter Transmission	0.82	100 nm Aluminium
Total instrument effective area	9.6 cm^2	100% of PSF
Instrument FOV	26.5° x 15.5°	For a flat detector plane at ~302 mm from centre of optic.